NMR Field-Cycling Study of Rotational Flow and Viscosity in Nematic Liquid Crystals

H. Gotzig, S. Grunenberg-Hassanein, and F. Noack

Physikalisches Institut der Universität Stuttgart, Pfaffenwaldring 57, D-70550 Stuttgart

Z. Naturforsch. **49a**, 1179–1187 (1994); received August 22, 1994

Dedicated to Professor Werner Müller-Warmuth on the occasion of his 65th birthday

A proton NMR method is described which enables rotational flow and viscosity measurements of low molecular weight nematic liquid crystals (NLC's). This is achieved by an extension of the common NMR field-cycling technique, namely by fast electronic switching of both the external magnetic field *direction* and *strength*. In thermodynamic equilibrium, the director of an NLC with positive diamagnetic anisotropy ($\Delta\chi > 0$) orients parallel to the external magnetic field. Thus a change of this direction causes a reorientation process of the molecules to align to the new equilibrium, which in low viscous systems in contrast to polymer liquid crystals is rather fast and hence requires fast field switching. We have studied systematically this response as a function of the initial field rotation angle θ_0 relative to the director for some homologous NLC's of the n-alkyl-cyanobiphenyl (nCB) series. It is shown that there exists a critical angle θ_{cr} in such a way that for $\theta_0 < \theta_{cr}$ the director rotation is homogeneous and only controlled by the rotational viscosity γ_1. For $\theta_0 > \theta_{cr}$, however (e.g. in the case of 5 CB θ_{cr} is ≈ 85 degrees) the viscoelastic behaviour is more complicated because of a coupling between flow and director gradients. The analysis of the alignment process by the changes of the proton line spectra also allows to determine the Leslie viscosities α_1, α_2, α_3, $\alpha_4 + \alpha_5$, and the average Frank elastic constant $\bar{K}$ by a single measurement.

Key words: Liquid crystals, Leslie viscosities, Rotational viscosity, NMR field-cycling, Flow measurements.

1. Aim of the Work

Nuclear magnetic resonance (NMR) spectroscopy has in recent years successfully been used to study flow processes in liquid crystals by changing the orientation of the external magnetic Zeeman field (flux density $\boldsymbol{B}$) relative to the crystal axis (director $\boldsymbol{n}$). The response can reveal characteristic details about the flow parameters of these materials. Up to the present, most of the NMR experiments were restricted to highly viscous polymer liquid crystals (PLC's), because in this case the director realignment is sufficiently slow to perform measurements by more or less conventional techniques [1–3].

Two main methods can be distinguished, namely a mechanical continuous or one-turn rotation of the sample perpendicular to the external field direction and on the other hand a rotation of the magnetic field by means of an electronic network. For both procedures NMR techniques, sometimes combined with optical methods, provide a precise tool to detect the realignment of the director.

Reprint requests to Prof. F. Noack.

Using the first mechanical approach, it was found for PLC's that the response flow to a transient turn of the director by an angle θ_0 depends on the magnitude of θ_0. There exists a critical angle $\theta_0 < \theta_{cr}$, which distinguishes homogeneous from inhomogeneous reorientation of the director. For $\theta_0 < 45°$ [1, 4] the flow is homogeneous and determined by the rotational viscosity γ_1, whereas experiments with rotation by an angle of about 90° [2, 4] show a one- or two-dimensional pattern formation, which is caused by the nonlinear coupling between the director motion and the viscous flow of the molecules (back-flow); this involves more than one of the liquid crystal viscosities. The effect is also seen by a reduction of the effective rotational viscosity $\gamma_{1\,\mathrm{eff}}$ [5]. To perform similar experiments with less viscous nematic liquid crystals (NLC's) it is necessary to apply the faster second approach. In common Zeeman fields with a magnetic flux density $\boldsymbol{B}$ of typically 1 T the realignment time is of the order of 30 ms for NLC's, but nearly 100 s for PLC's. In this paper it is shown that the NMR field-cycling technique, through the possibility of switching the angle θ_0 between the director $\boldsymbol{n}$ and the Zeeman field $\boldsymbol{B}_\theta$ in a few milliseconds, allows to realize adequately fast switch-

0932-0784 / 94 / 1200-1179 $ 06.00 © – Verlag der Zeitschrift für Naturforschung, D-72027 Tübingen

ing conditions for measurements of low viscous liquid crystals.

2. Experimental Techniques

2.1 NMR Apparatus

The NMR field-cycling technique has generally been used to determine the frequency dependence of longitudinal proton or deuteron relaxation times T_1, and both the method and numerous results are described in several reviews [6–8]. In order to perform rotational flow measurements we had to modify our proton field-cycling spectrometer [6] (i) to allow switching of both the external magnetic field *direction* and *strength*, and (ii) to allow a spectral signal analysis by Fast Fourier Transform (FFT) data processing. For the first purpose the cylindrical Zeeman field coil of the proton field-cycling spectrometer with a maximum field of 0.2 T in z-direction was extended by a saddle coil [9, 10] inside the cylinder bore with a maximum field of 0.06 T in x-direction as shown in Figure 1. The current through the transverse coil is controlled by a 3 kW commercial power supply (Delta Elektronika), which is switchable within 5 ms. The z-field, switchable in about 1 ms, is regulated by a homebuild GTO network described previously [6]. By varying the magnetic flux density in both the z- and x-direction any angle $0° < \theta_0 < 90°$ relative to the z-direction could be adjusted in about 5 ms up to a field of 0.06 T. Details are given in [11]. For the second purpose the field-cycling spectrometer was interfaced to a PC with a two-channel FFT. At present we use a Larmor frequency $\nu_0 = 8.9$ MHz. A typical NLC spectrum has a width of 100 kHz, the resolution of our apparatus by the magnet inhomogeneity is about 300 Hz. The data were recorded with a sampling time of 2 μs and the FFT was performed with 4096 complex signal points.

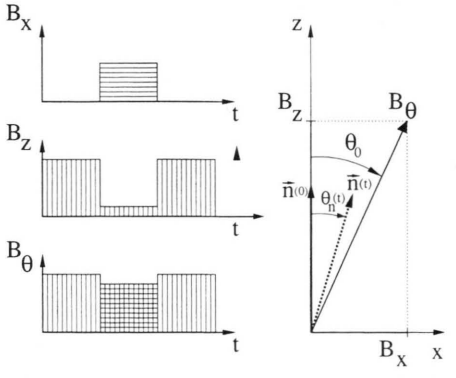

Fig. 1. Principle of the angular dependent fast field-cycling NMR method for flow or relaxation measurements, where the orientation of the NMR Zeeman field B_θ is cycled periodically relative to selected axis, in this case the liquid crystal director $\boldsymbol{n}$.

The principle of a measuring cycle is shown in Figure 2. It can be separated into 3 periods: The *first period* I creates the thermodynamic equilibrium of both the magnetization $\boldsymbol{M}$ and the director field $\boldsymbol{n}$, which means that $\boldsymbol{n}$ in the NLC becomes parallel to the field $B_z(\theta_n = 0)$, and in good approximation $\nabla \boldsymbol{n} = 0$. At time $t = \tau_0$ the *second period* II starts. Here the field in z-direction is switched to a lower value B_z, while at the same time the field in x-direction is switched to a value B_x to produce an inclination of the total field

$$|\boldsymbol{B}_\theta| = \sqrt{B_x^2 + B_z^2} \tag{1}$$

by an angle

$$\theta_0 = \arctan\left(\frac{B_x}{B_z}\right) \tag{2}$$

relative to the director $\boldsymbol{n}$. This is a nonequilibrium configuration and a reorientation process will start, where θ_n will approach θ_0. It is measured in the *detection period* III beginning at time $t = \tau_R$. After a short time delay δt, which is necessary to improve the field stability, an NMR free-induction-decay (FID) is created with a $\pi/2$ rf-pulse B_1 and transformed by FFT to give a proton spectrum, where the flow becomes observable through the separations and amplitudes of the individual lines. If $\theta_0 < \theta_{cr}$ it is advantageous to extend the interval to $\delta t \approx 2\,T_1$, where T_1 is the proton spin relaxation time, in order to increase the magnetization. This implies that the original flow time has to be corrected by the delay.

By varying the length of the second period from typically 0 to 100 seconds the form of the spectrum changes due to the increasing angle θ_n between the local director $\boldsymbol{n}$ and the magnetic detection field B_z, and this development was recorded in usually 40 steps. Both the dependence of the line splitting and of the full profile of the spectrum $f(\nu)$ on τ_R are characteristic for the flow of the molecules, in particular the spectrum allows to distinguish a *homogeneous* from an *inhomogeneous* process. In addition, the equilibrium spectrum $f_0(\nu)$ for $\theta_n = 0$, corresponding to $t = \tau_0$, was recorded. The accuracy of the angle adjustment varies

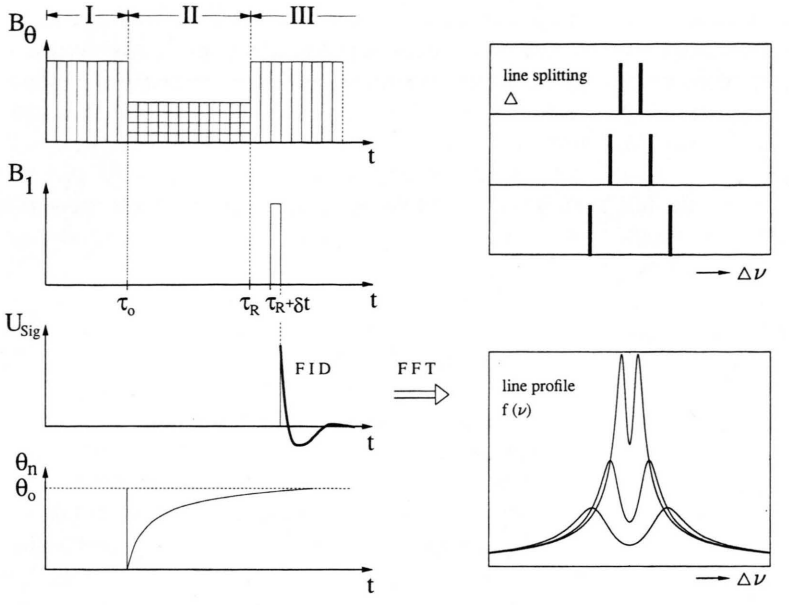

Fig. 2. Polarisation-, flow- and detection-periods (I, II, III) of the angular dependent fast field-cycling NMR method for flow measurements in liquid crystals (left side, top), and the related rf-field irradiation $B_1(t)$, signal amplitude $U_{Sig}(t)$ and director orientation $\theta_n(t)$ (left side, lower drawings). The right side of the diagram shows schematically the time dependent variation of the line splitting and the full proton spectrum obtained by FFT of $U_{Sig}(t)$.

from a few degrees at small θ_0 to less than 1 degree near $\theta_0 = 90°$.

The director reorientation was studied for both different temperatures T (from the clearing point T_C to $T_C - 8\,°C$) and different starting angles θ_0 (40, 70, and 88°).

2.2 Data Handling

In the simple case where the sample contains only one type of proton spin pairs with a separation r_{12} and an orientation β_{12} relative to the external detection field B_z, the spectrum consists of two lines with a splitting [12]

$$\Delta = \frac{3\gamma^2\hbar}{2r_{12}^3}(3\cos^2\beta_{12} - 1), \tag{3}$$

as illustrated by Fig. 2, where γ is the gyromagnetic ratio of the protons. In a liquid crystal the prefered axis is the director $\boldsymbol{n}$, and the angle β_{12} can be expressed by the angle θ_n between the director and the field B_z, the angle ϑ between the average molecular axis and the director, and the average angle φ_{12} between the spin pair axis and the molecular axis. According to Schmiedel et al. [13] this gives

$$\Delta = \frac{3\gamma^2\hbar}{8r_{12}^3}\frac{1}{2}(3\cos^2\theta_n - 1)\,\langle(3\cos^2\vartheta - 1)\rangle \cdot \langle(3\cos^2\varphi_{12} - 1)\rangle, \tag{4}$$

where

$$S \equiv \frac{1}{2}\langle(3\cos^2\vartheta - 1)\rangle \tag{5}$$

is the nematic order parameter, and similarly the field direction is often characterized by another order parameter

$$S_B \equiv \frac{1}{2}(3\cos^2\theta_n - 1). \tag{6}$$

Since the real sample contains different spin pairs, and the orientation of the director is not necessarily homogeneous over the whole sample, the observable spectrum $f(\nu)$ is a superposition of the individual contributions of all spin pairs, which can be written in the form [14]

$$f(\nu) = \int_0^{\theta_0} P(\theta_n)\frac{1}{S_B} f_0\left(\frac{\nu}{S_B}\right) d\theta_n, \tag{7}$$

where $P(\theta_n)$ means the probability density function of the director orientation in the sample. In the case of $\theta_0 < \theta_{cr}$ this is a δ-function. A schematic drawing of (7) is shown by the line profiles in Fig. 2 to distinguish this case from the simple treatment by (3). The form of (7) essentially agrees with the more recent result of Spiess et al. [2] for the analysis of deuteron spectra in flow experiments. However, in the following we use explicitly calculated expressions for $P(\theta_n)$, rather than numeric approximations.

In order to compare the experimental data with the spectral profiles of (3) or (7), respectively, we did the following. If there exists only one well-resolved splitting and if $\theta_0 < \theta_{cr}$, so that the director reorientation is homogeneous, the flow of the molecules can be completely controlled by the time dependence of Δ. In the more general case, for instance if $\theta_0 > \theta_{cr}$, the full spectral profile of (7) has been considered. The simulation of $f(\nu)$ was performed by using the measured $f(\nu)$ spectrum together with calculated forms of $P(\theta_n)$ based on the one- and two-dimensional director distributions introduced by Martins [1] and Spiess [2]. In the one-dimensional case we obtained

$$P(\theta_n) = \frac{2}{\varepsilon \pi} \frac{1}{\theta_n \left(\frac{\theta_n}{\theta_{max}}\right)^{-\frac{1}{\varepsilon}} \sqrt{1 - \left(\frac{\theta_n}{\theta_{max}}\right)^{\frac{2}{\varepsilon}}}}, \quad (8)$$

and in the two-dimensional case

$$P(\theta_n) = \frac{8}{\pi^2} \frac{\left(\frac{\sin\theta_n}{\sin\theta_{max}}\right)^{\frac{1}{\varepsilon}}}{\varepsilon \tan\theta_n \sqrt{1 - \left(\frac{\sin\theta_n}{\sin\theta_{max}}\right)^{\frac{2}{\varepsilon}}}} \cdot \int_0^{\arccos\left[\left(\frac{\cos\theta_n}{\cos\theta_{max}}\right)^{\frac{1}{2\varepsilon}}\right]} \frac{d\xi}{\sqrt{1 - \left[1 - \frac{\sin\theta_n}{\sin\theta_{max}}\right]^{-\frac{2}{\varepsilon}} \sin^2\xi}}, \quad (9)$$

as demonstrated in the Appendix. The two involved model parameters θ_{max} and ε for the maximum amplitude and the deformation of the director field were optimized as a function of the flow time $\tau_R - \tau_0$ in the detection period (seeFig. 2) by a minimalization of the deviation between the simulated and the experimental spectrum. Such a simulation treats 512 points of the amplitude spectrum. The line broadening of ≈ 300 Hz originating from the inhomogeneity of the field-cycling magnet was taken into account by an angle-independent broadening term in the spectrum.

2.3 Samples

Homologous liquid crystals of the 4-n-alkoxy-4′-cyano-biphenyl series, namely 5CB, 6CB, 7CB and 8CB, were purchased from Merck and filled in quarz-glass-tubes with an inner diameter of 8 mm and a length of 10 mm by the normal freeze-pump-thaw technique. All these materials are nematic near or slightly above room temperature. In order to treat the temperature dependencies relative to the clearing point T_C, the absolute sample temperatures T were scaled by $T = T_C - \Delta T$, and the clearing point was determined for every material with an accuracy of $\approx 0.2\,^\circ$C (5CB: 35.2 °C, 6CB: 28.6 °C, 7CB: 39.5 °C, 8CB: 40.3 °C). During the flow experiments the sample temperature was maintained constant within $\approx 0.2\,^\circ$C.

3. Experimental Results

3.1 Angular Dependent Line Splitting Δ and Spectrum $f(\nu)$

Using the field-cycling technique described before, the line splittings and the full spectra of several liquid crystals were determined for different starting angles θ_0 of the reorientation process towards equilibrium. The different procedures are illustrated for 5CB by Figures 3, 4, and 5. The equilibrium spectrum of 5CB with typically two nearly equal line splittings Δ_I and Δ_0 is shown in Fig. 3 (insert). The measurement of the flow was generally performed on the outer lines with splitting $\Delta \equiv \Delta_0$, because near the magic angle the resolution is higher. Results from Δ_I are the same, but with larger error bars. The main Fig. 3 only represents the variation of Δ as a function of $\tau_R - \tau_0$ for the initial rotation $\theta_0 = 40°$ at 30 °C. The related variations of the complete spectrum $f(\nu)$ for different initial rota-

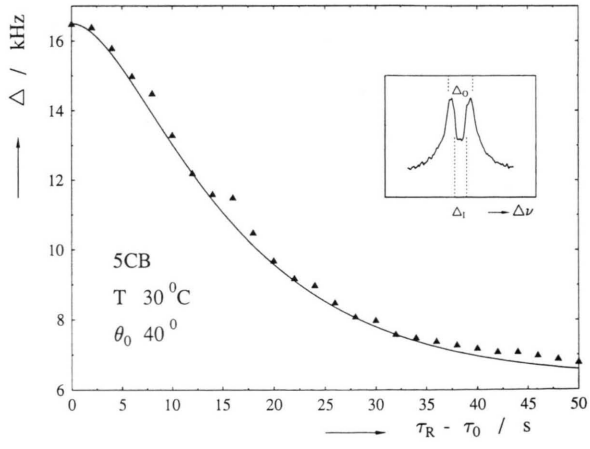

Fig. 3. Time dependence of the outer line splitting $\Delta \equiv \Delta_0$ for 5CB at $T = 30\,^\circ$C in the flow field and model fit by (10). The inset shows the definition of the inner and outer splittings Δ_I and Δ_0, respectively.

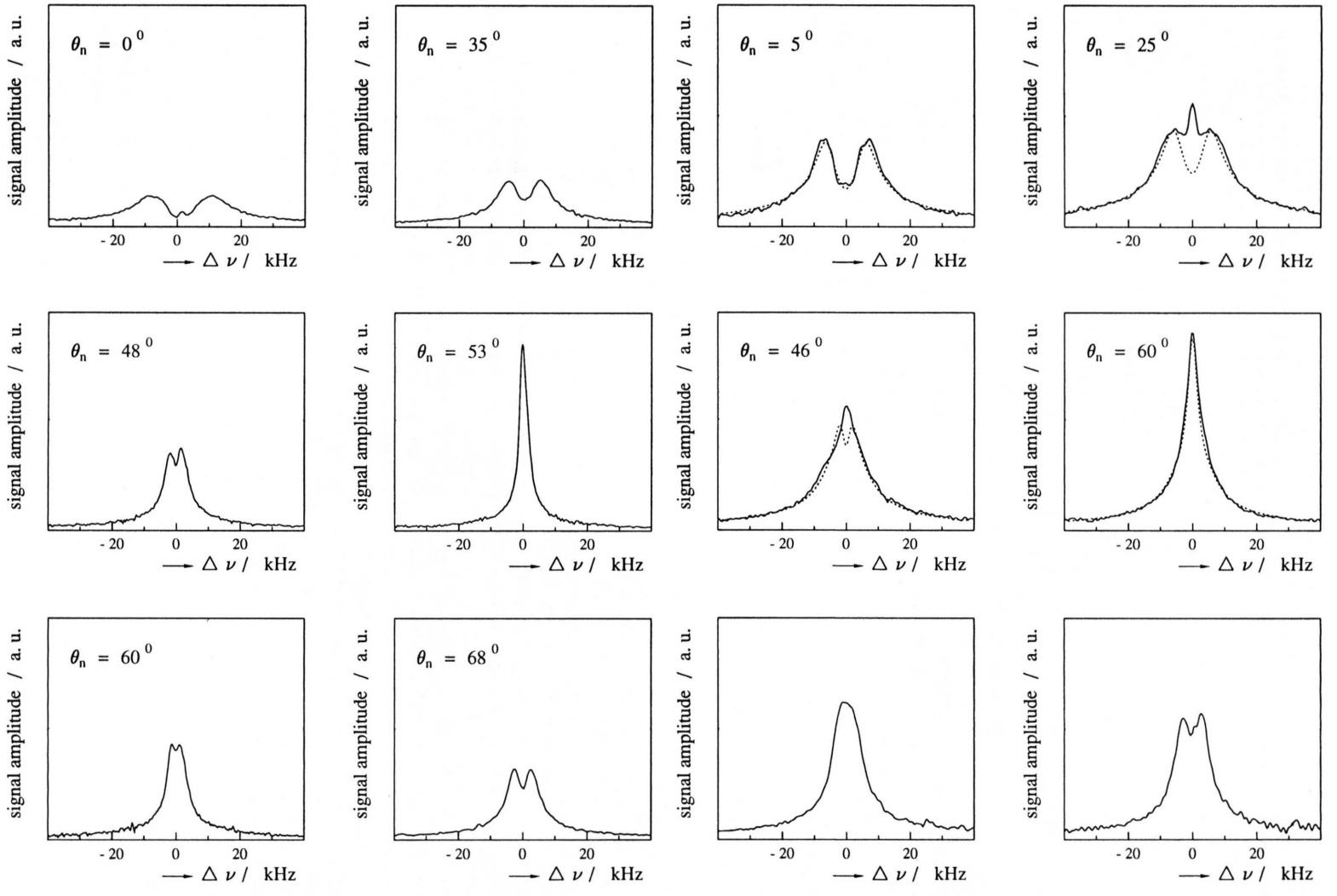

Fig. 4. Development of the 5CB proton spectrum after an initial field rotation switch of $\theta_0 = 70°$ at 27.5 °C (homogeneous flow) for 6 values of the director orientation θ_n. The abscissa $\Delta\nu$ measures the frequency relative to the central Larmor frequency $\nu_0 = 8.9$ MHz of the spectrometer, the amplitudes U are linear, arbitrary units. The original equilibrium spectrum is a broad dublett, which dramatically narrows when approaching the magic angle. For larger angles the spectrum transforms to a 3 times narrower dublett than the equilibrium spectrum.

Fig. 5. Development of the 5CB proton spectrum after an initial field rotation switch of $\theta_0 = 88°$ at 33.5 °C (inhomogeneous flow) for 6 values of the director orientation θ_n. Different from Fig. 4 there grows a central line in the spectrum before θ_n reaches the magic angle, the magic angle spectrum is broader by a factor of 2.5 than for the homogeneous director flow. The final state is again a dublett. The dotted lines are model simulations by (7), (9) to illustrate the model quality.

tions θ_0, namely for $\theta_0 = 70$ and $\theta_0 = 88°$, i.e. for one value *below* and one *near* the critical angle θ_{cr}, are shown in Figs. 4 and 5. The essential aspects of these data are the following:

- The line splitting follows the well-known arctan-law [16]:

$$\Delta = \frac{3\,\Delta_{max}}{2} \cdot \left[\cos^2\left[\theta_0 - \arctan\left\{\tan\theta_0\, e^{\left(-\frac{\tau_r - \tau_0}{T_R}\right)}\right\}\right] - \frac{1}{3}\right] \tag{10}$$

  with time constant T_R as expected from the Leslie-Ericksen-theory [16] in the case of $\theta_0 < \theta_{cr}$; Δ_{max} denotes the equilibrium line splitting.
- The variation of the full spectrum for $\theta_0 < \theta_{cr}$ involves via $P(\theta_n) = \delta(\theta_n - \theta_{max})$ in (7) the same time constant T_R according to

$$\theta_n = \theta_0 - \arctan\left[\tan\theta_0\, e^{\left(-\frac{\tau_r - \tau_0}{T_R}\right)}\right]. \tag{11}$$

  But the full spectrum allows to observe the flow more critically at angles between 40 to 60°, where the line splitting becomes too small to be resolved.
- For angles $\theta_0 > \theta_{cr}$, it was no longer possible to simulate the angular development of all the experimental spectra in Fig. 5 with the considered model relations using only one single averaged spin pair. The value θ_{cr} depends on instrumental parameters like the strength and inhomogeneity of the field as well as on the size and the purity of the sample. In some cases θ_{cr} was found near 40°, in others as 5CB near 85° [15].

The observed time constants T_R and initial splittings Δ_{max} are listed in Table 1 for all studied materials. The time constants are the basis for the evaluation of the rotational viscosities γ_1. Neglecting some discrepancies of the spectrum simulation for large initial field rotations, it is also possible to use the formalism to determine the three Leslie viscosities $\alpha_1, \alpha_2, \alpha_3$ individually, the sum $\alpha_4 + \alpha_5$, and also the average Frank elastic constant $\bar{K}$.

3.2 *Evaluation of the Rotational Viscosity* γ_1 and $\gamma_{1\,eff}$

From the balance between the magnetic and the frictional torque on $\boldsymbol{n}$ in the reorientation field B_θ together with the time constant T_R follows for the homogeneous flow the rotational viscosity γ_1 by the relation [16]

$$\gamma_1 = \frac{T_R\,\Delta\chi\,B_\theta^2}{\mu_0}, \tag{12}$$

where $\Delta\chi$ is the diamagnetic anisotropy and μ_0 the vacuum permeability. If the director flow is inhomogeneous, i.e. $\theta_0 > \theta_{cr}$, (12) was still observed to be valid [1] in the initial phase of the time dependent splitting for the reorientation process according to (10), if γ_1 is replaced by an effective rotational viscosity $\gamma_{1\,eff}$. Values of $\Delta\chi$ were taken from [17–19], B_θ was determined using a Bell Gauss-meter with an accuracy of $\pm 1\%$. The evaluated values of γ_1 and $\gamma_{1\,eff}$ are listed for several temperatures in Table 1. From the experimental scatter, the error limits were estimated to be $\pm 10\%$. Some remarks about the differences between the two viscosities are given in Chapter 4.2.

Table 1. Rotational viscosities γ_1 and $\gamma_{1\,eff}$ of the *n*-CB series for $n = 5, 6, 7$, and 8 at different temperatures ΔT relative to the clearing point T_C. Also shown are the directly measured quantities T_R and Δ_{max} (see (10) and (11)).

ΔT/K		5CB	6CB	7CB	8CB
0.5	T_R/s				4.7
	γ_1/Pa s				0.029
	$\gamma_{1\,eff}$/Pa s				
	Δ_{max}/kHz				15.0
1	T_R/s		7.8	6.3	5.3
	γ_1/Pa s		0.048	0.033	0.033
	$\gamma_{1\,eff}$/Pa s				
	Δ_{max}/kHz		14.3	16.1	15.1
2	T_R/s	4.9	8.7	7.0	6.2
	γ_1/Pa s	0.033	0.058	0.042	0.043
	$\gamma_{1\,eff}$/Pa s	0.033			
	Δ_{max}/kHz	14.2	15.7	17.2	18.7
4	T_R/s	5.5	10.7	7.5	7.2
	γ_1/Pa s	0.042	0.08	0.052	0.056
	$\gamma_{1\,eff}$/Pa s	0.041			
	Δ_{max}/kHz	15.0	17.2	19.0	21.3
6	T_R/s	6.6	13.5	8.2	10.2
	γ_1/Pa s	0.054	0.108	0.061	0.084
	$\gamma_{1\,eff}$/Pa s	0.052			
	Δ_{max}/kHz	18.6	18.1	20.3	23.1
8	T_R/s	7.8			
	γ_1/Pa s	0.067			
	$\gamma_{1\,eff}$/Pa s	0.065			
	Δ_{max}/kHz	19.7			

3.3 *Evaluation of the Leslie Viscosities* α_1, α_2, α_3, $\alpha_4 + \alpha_5$, *and the Average Frank Elastic Constant* $\bar{K}$

As mentioned before, our measurements do not yet allow a quantitative description of the full reorienta-

tion process by (7) in combination with (8)–(11). However, if we overlook some details of the spectrum and consider the Martins formalism for the time evolution of θ_n according to the planar Leslie-Ericksen equation [1]

$$\left[\gamma_1 - \frac{j^2(\theta_n)}{g(\theta_n)}\right]\frac{\partial\theta_n}{\partial t} - \frac{\Delta\chi\, B_\theta^2}{2\mu_0}\sin 2(\theta_0-\theta_n) - K(\theta_n)=0 \tag{13}$$

with

$$j(\theta_n)=\alpha_2-(\alpha_2+\alpha_3)\sin^2(\theta_0-\theta_n), \tag{13a}$$

$$g(\theta_n)=(\alpha_1\cos^2(\theta_0-\theta_n)+\alpha_2+\alpha_3)\sin^2(\theta_0-\theta_n) + \tfrac{1}{2}(\alpha_4+\alpha_5-\alpha_2), \tag{13b}$$

and

$$K(\theta_n)=\bar{K}\frac{\partial^2\theta_n}{\partial z^2} \tag{13c}$$

instead of the simple arctan-law (11), it becomes possible to estimate in addition to $\gamma_1=\alpha_3-\alpha_2$ the Leslie viscosities $\alpha_1, \alpha_2, \alpha_4+\alpha_5$, as well as the average Frank elastic constant $\bar{K}$. Our approximation implies to restrict θ_n to angles $< 50°$ and to neglect on one hand the time dependence of the deformation parameter ε in (8), and on the other hand the inner line which occurs during the intermediate reorientation process (see Fig. 5 at $\theta_n \approx 25°$).

The solution of the Leslie-Ericksen relation and the fitting of the experimental data to the theoretical model was done with the fitting program Scientist for ordinary differential equations (Micromath); the spectra simulations were performed on a Unix-PC. Table 2 lists the obtained optimized parameters for 5CB.

Table 2. Leslie viscosities α_i and average Frank elastic constant $\bar{K}$ for 5CB at $T=33.5\,^\circ$C determined by the inhomogeneous flow measurement of this work. The evaluation of (13), (13a), (13b), (13c) is sketched in the text. For comparison some data from the literature [20] are included.

α_1/Pa s	α_2/Pa s	α_3/Pa s	$\alpha_3+\alpha_5$/Pa s	$\bar{K}$/N	Ref.
0.042	−0.036	−0.003	0.08	$2\cdot10^{-12}$	This work
—	−0.042	≅0	0.072	—	Chmielewski [20]

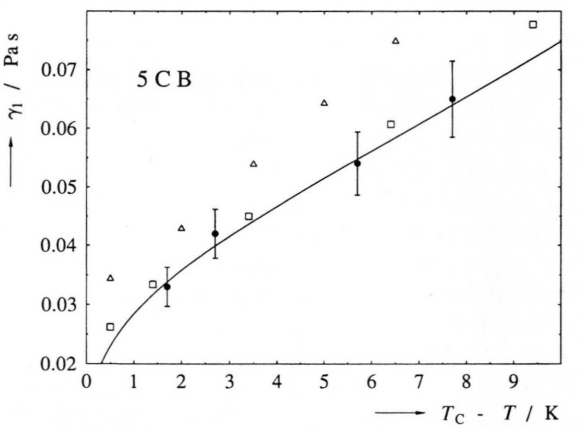

Fig. 6. Temperature dependence of the rotational viscosity γ_1 for 5CB. (●): Measurements of this work. Full line: Model fit by (14) and (15) with parameters listed in Table 2. (□): Measurements of [23] (△): Measurements of [20].

4. Discussion and Conclusions

4.1 Rotational Viscosity

Our results on γ_1 and $\gamma_{1\,\mathrm{eff}}$ essentially support the viscosity data available in the literature for 5CB, 6CB and 8CB [20–25] but reveal considerable discrepancies up to an order of magnitude of 7CB [26]. The two situations are illustrated by Figs. 6 and 7, which compare the temperature dependence of γ_1 for 5CB and 7CB of our field-cycling studies with data from the literature. The full lines are model fits of the frequently used expression for γ_1, namely [27]

$$\gamma_1(T)=AS^2\exp\left(\frac{E}{kT}\right) \tag{14}$$

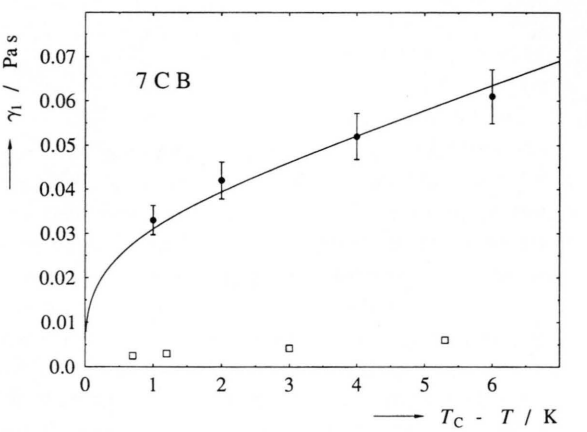

Fig. 7. Temperature dependence of the rotational viscosity γ_1 for 7CB. (●): Measurements of this work. Full line: Model fit by (14) and (15) with parameters listed in Table 2. (□): Measurements of [26].

Table 3. Optimized parameters obtained by temperature dependent model fits of (14) and (15) to the measured rotational viscosities for the *n*-CB series.

	5CB	6CB	7CB	8CB
$A/\mathrm{Pa\,s}$	$2.3 \cdot 10^{-7}$	$1.9 \cdot 10^{-7}$	$9.7 \cdot 10^{-7}$	$5.5 \cdot 10^{-8}$
$E/\frac{\mathrm{kJ}}{\mathrm{mol}}$	34	36	31	39
β	0.141	0.142	0.145	0.148

with the order parameter approximation

$$S = \left(1 - \frac{T}{T_C}\right)^{\beta}. \tag{15}$$

The optimized parameters (pre-exponential factor A, activation energy E, temperature exponent β) are given for all materials in Table 3.

The essential point of our new viscosity measurements is that the homogeneity of the flow implied by (7) can be quantitatively checked by the evolution of the proton spin spectrum and is not an unproved asssumption. This is a decisive point since the angle θ_{cr} where the flow type changes to inhomogeneous, obviously deviates from the theoretical expectation $\theta_{cr} \approx 45°$ [1, 2]. Further, and in contrast to the results of Magnuson et al. [28] it is not observed for 5CB with $\theta_0 < \theta_{cr}$ that different parts of the molecule (e.g. chains and aromatic rings) rotate significantly differently. The absence of separate flow components is most reliably seen by the form of the spectrum when θ_n approaches the magic angle, since in this case only one single line develops, corresponding to one single value of θ_n.

4.2 Leslie Viscosities

The validity of (13) for flow experiments after creating a nonequilibrium between the magnetic field and the nematic director orientation is still disputed because of the in-plane assumption of the director motion and the possibly incomplete Martins-Spiess-Ansatz for inhomogeneous director distributions (see Appendix). Nevertheless there exist several results for PLC's based on this approach [29], but so far no independent control measurements. A similar theoretical basis has recently been proposed and applied for PLC's by Moscicki et al. [30], who have switched an electric instead of a magnetic field direction. A characteristic result of these methods is the relatively small value of $\eta_b \equiv \frac{1}{2}(\alpha_2 + 2\alpha_3 + \alpha_4 + \alpha_5)$ compared with α_3 so that

$$\gamma_{1\,\mathrm{eff}} \approx \gamma_1 - \frac{2\alpha_3^2}{\alpha_2 + 2\alpha_3 + \alpha_4 + \alpha_5} \tag{16}$$

becomes rather different from γ_1. This has been verified experimentally both in electric and magnetic flow experiments of PLC's [1, 2, 30].

In case of the present measurements on NLC's the results about the α_i's can be compared with independent, more direct experimental viscosity studies. For 5CB several Leslie viscosities have been reported by Chmielewski [20] and Skarp et al. [21]. We found that the agreement is satisfactory within the experimental error limits of maximum an order of magnitude for α_3 and minimum $< 10\%$ for α_2. In particular the negligible difference between γ_1 and $\gamma_{1\,\mathrm{eff}}$ (Table 2), i.e. between the rotational viscosity observed in the flow for small and larger director rotations, is understandable because of the small α_3 to η_b ratio compared with γ_1. However, we once again emphasize that the proton spectrum observed during the flow process is not in quantitative agreement with the model equations (7), (8), (9), and (13).

Acknowledgements

The authors thank Dipl.-Phys. J. Struppe for many helpful discussions. Financial support by the Deutsche Forschungsgemeinschaft is gratefully acknowledged.

5. Appendix

5.1 One-Dimesional Director Distribution

From the one-dimensional inhomogeneous director distribution in z-direction introduced by Martins

$$\theta_n(z,t) = \theta_{\max}(t)\cos^{\varepsilon}(q_z z), \tag{17}$$

where $\theta_{\max}(t)$ is the maximum time depended distortion and q_z is the related wave vector, and the definition of $P(\theta_n)$ in (7),

$$P(\theta_n) = N * \left[\frac{\partial}{\partial z}\theta_n\right]^{-1}, \tag{18}$$

where N is the normalisation factor, follows

$$P(\theta_n) = N * [-q_z \theta_{\max} \varepsilon \sin(q_z z) \cos^{\varepsilon-1}(q_z z)]^{-1} \quad (19)$$
$$= N * \left[-q_z \varepsilon \theta_n \left(\frac{\theta_n}{\theta_{\max}}\right)^{-\frac{1}{\varepsilon}} \left\{1 - \left(\frac{\theta_n}{\theta_{\max}}\right)^{\frac{2}{\varepsilon}}\right\}^{\frac{1}{2}} \right]^{-1}.$$

Normalising $P(\theta_n)$ to 1 finally gives

$$P(\theta_n) = \frac{2}{\varepsilon \pi} \frac{1}{\theta_n \left(\frac{\theta_n}{\theta_{\max}}\right)^{-\frac{1}{\varepsilon}} \sqrt{1 - \left(\frac{\theta_n}{\theta_{\max}}\right)^{\frac{2}{\varepsilon}}}}. \quad (20)$$

5.2 *Two-Dimensional Director Distribution*

From the two-dimensional director distribution function in x and z-direction introduced by Spiess

$$\sin\theta_n(x, z, t) = \sin\theta_{\max}(t) \sin^{\varepsilon}(q_x x) \sin^{\varepsilon}(q_z z), \quad (21)$$

where q_x and q_z are the wave vector in x- and z-direction of the time dependent director distortion, and the definition of $P(\theta_n)$ in (7),

$$P(\theta_n) = N * \frac{1}{|\nabla_r \theta|_{\theta_n = \text{const}}} \quad (22)$$

cannot be evaluated in a closed form as (18). However, considering the areas of constant θ_n-inclination on the $\theta_n(x, z, t)$ surface one can approximately express $P(\theta_n)$ as the difference of two neighbouring projections for constant θ_n in the x-z-plane, which gives

$$P(\theta_n) = N \frac{\left(\frac{\sin\theta_n}{\sin\theta_{\max}}\right)^{\frac{1}{\varepsilon}}}{\varepsilon \tan\theta_n} \cdot \int_0^{\arccos\left[\left(\frac{\cos\theta_n}{\cos\theta_{\max}}\right)^{\frac{1}{2\varepsilon}}\right]} \frac{d\xi}{\sqrt{\cos^2\xi - \left(\frac{\sin\theta_n}{\sin\theta_{\max}}\right)^{\frac{2}{\varepsilon}}}}. \quad (23)$$

N is a normalisation constant and $\xi = q_x x$ an integration variable. Normalisation $P(\theta_n)$ to 1 finally gives

$$P(\theta_n) = \frac{8}{\pi^2} \frac{\left(\frac{\sin\theta_n}{\sin\theta_{\max}}\right)^{\frac{1}{\varepsilon}}}{\varepsilon \tan\theta_n \sqrt{1 - \left(\frac{\sin\theta_n}{\sin\theta_{\max}}\right)^{\frac{2}{\varepsilon}}}} \cdot \int_0^{\arccos\left[\left(\frac{\cos\theta_n}{\cos\theta_{\max}}\right)^{\frac{1}{2\varepsilon}}\right]} \frac{d\xi}{\sqrt{1 - \left[1 - \frac{\sin\theta_n}{\sin\theta_{\max}}\right]^{-\frac{2}{\varepsilon}} \sin^2\xi}}, \quad (24)$$

which is an elliptic integral of the first kind.

[1] A. F. Martins, P. Esnault, and F. Volino, Phys. Rev. Lett. **57,** 1745 (1986).
[2] N. Schwenk and H. W. Spiess, J. Phys. II France **3,** 865 (1993).
[3] D. A. Grabowski and C. Schmidt, Macromolecules **27,** 2632 (1994).
[4] J. P. Casquilho, P. Esnault, and F. Volino, Mol. Cryst. Liq. Cryst. **180 B,** 343 (1990).
[5] E. Guyon, R. Meyer, and J. Salan, Mol. Cryst. Liq. Cryst. **54,** 261 (1979).
[6] F. Noack, Prog. NMR Spectrosc. **18,** 171 (1986).
[7] R. Kimmich, Bull. Magn. Res. **1,** 195 (1980).
[8] S. H. Koenig and R. D. Brown, Prog. NMR Spectrosc. **22,** 487 (1990).
[9] K. Beyerle, Arch. Elektrotechnik **25,** 267 (1931).
[10] R. E. Richards and D. I. Hoult, J. Magn. Res. **24,** 71 (1976).
[11] J. Struppe and F. Noack (in prep.).
[12] G. E. Pake, J. Chem. Phys. **16,** 327 (1948).
[13] H. Schmiedel, B. Hillner, S. Grande, A. Lösche, and St. Limmer, J. Magn. Res. **40,** 369 (1980).
[14] A. Frieser, H. Schmiedel, B. Hillner, and A. Lösche, Mol. Cryst. Liq. Cryst. **109,** 245 (1984).
[15] J. Mager, Thesis, Universität Stuttgart 1993.
[16] P. G. de Gennes, The Physics of Liquid Crystals, Clarendon Press, Oxford 1974.
[17] A. Buka and W. H. de Jeu. J. Physique **43,** 361 (1982).
[18] P. L. Sherrell and D. A. Crellin, J. Physique **40,** C3-211 (1979).
[19] N. V. Madhusudana and R. Pratibha, Mol. Cryst. Liq. Cryst. **89,** 249 (1982).
[20] A. G. Chmielewski, Mol. Cryst. Liq. Cryst. **132,** 339 (1986).
[21] K. Skarp, S. T. Lagerwall, and B. Stebler, Mol. Cryst. Liq. Cryst. **60,** 215 (1980).
[22] H. Kneppe, F. Schneider, and N. K. Sharma, Ber. Bunsenges. Phys. Chem. **85,** 784 (1981).
[23] H. Kneppe, F. Schneider, and N. K. Sharma, J. Chem. Phys. **77,** 3203 (1982).
[24] F.-J. Bock, H. Kneppe, and F. Schneider, Liq. Cryst. **1,** 239 (1986).
[25] J. Constant and E. P. Raynes, Mol. Cryst. Liq. Cryst. **62,** 115 (1980).
[26] P. Chattopadhyay and S. K. Roy, Mol. Cryst. Liq. Cryst. **237,** 1 (1993).
[27] S. T. Wu and C. S. Wu, Liq. Cryst. **8,** 171 (1990).
[28] M. L. Magnuson and B. M. Fung, J. Chem. Phys. **100,** 1470 (1994).
[29] J. P. Casquilho, Thesis, Universidade Nova de Lisboa, Portugal, 1989.
[30] A. Kozak, G. P. Simon, J. K. Moscicki, and G. Williams, Mol. Cryst. Liq. Cryst. **193,** 155 (1990).